# EESM-Based Link Adaptation in Point-to-Point and Multi-Cell OFDM Systems: Modeling and Analysis

Jobin Francis and Neelesh B. Mehta, *Senior Member, IEEE*

*Abstract*—In contemporary wideband orthogonal frequency division multiplexing (OFDM) systems, such as Long Term Evolution (LTE) and WiMAX, different subcarriers over which a codeword is transmitted may experience different signal-to-noise-ratios (SNRs). Thus, adaptive modulation and coding (AMC) in these systems is driven by a vector of subcarrier SNRs experienced by the codeword, and is more involved. Exponential effective SNR mapping (EESM) simplifies the problem by mapping this vector into a single equivalent flat-fading SNR. Analysis of AMC using EESM is challenging owing to its non-linear nature and its dependence on the modulation and coding scheme. We first propose a novel statistical model for the EESM, which is based on the Beta distribution. It is motivated by the central limit approximation for random variables with a finite support. It is simpler and as accurate as the more involved ad hoc models proposed earlier. Using it, we develop novel expressions for the throughput of a point-to-point OFDM link with multi-antenna diversity that uses EESM for AMC. We then analyze a general, multi-cell OFDM deployment with co-channel interference for various frequency-domain schedulers. Extensive results based on LTE and WiMAX are presented to verify the model and analysis, and gain new insights.

*Index Terms*—Orthogonal frequency division multiplexing (OFDM), adaptive modulation and coding, exponential effective SNR mapping (EESM), scheduling, cell throughput, co-channel interference, beta distribution.

## I. INTRODUCTION

**H**IGH data rate requirements coupled with scarcity of the spectrum have driven the quest for techniques that improve spectral efficiency. One important technique for doing so is adaptive modulation and coding (AMC). In it, the transmitter chooses its modulation and coding scheme (MCS) from a finite set of MCSs depending on the channel conditions while satisfying a constraint on the probability of error. AMC is an integral part of current and next generation wireless systems such as Long Term Evolution (LTE) and IEEE 802.16e/m WiMAX. These systems are wideband in nature and use orthogonal frequency division multiplexing (OFDM).

In a practical OFDM system, however, AMC is not done on a per-subcarrier basis because of its significant feedback and control signaling overhead. Instead, the same MCS is used on all the subcarriers assigned to a user. Due to the

frequency-selective nature of the wideband channel, the signal-to-noise-ratios (SNRs) of these subcarriers can be different. These subcarriers can even span multiple coherence bandwidths. Thus, the MCS chosen is a function of a vector of subcarrier SNRs. In principle, this requires an unwieldy multi-dimensional lookup table to map the vector of SNRs to the MCS, which is cumbersome to generate and store, and is seldom used [1]. Therefore, link quality metrics (LQMs) have been proposed to simplify this problem and make it similar to AMC over narrowband channels, in which a simple, one-dimensional lookup table suffices [2, Chap. 9].

A popular and accurate LQM is exponential effective SNR mapping (EESM) [3]. It maps the vector of subcarrier SNRs seen by the codeword into an effective SNR. If $\gamma_i$ denotes the SNR of the $i^{\text{th}}$ subcarrier, for $1 \leq i \leq N_{\text{sc}}$, then the effective SNR using EESM $\gamma_{\text{eff}}^{(m)}$ for MCS $m$ when transmitted over these $N_{sc}$ subcarriers is defined as

$$\gamma_{\text{eff}}^{(m)} = -\beta_m \ln\left(\frac{1}{N_{\text{sc}}} \sum_{i=1}^{N_{\text{sc}}} \exp\left(-\frac{\gamma_i}{\beta_m}\right)\right), \quad (1)$$

where $\beta_m > 0$ is an MCS-dependent scaling parameter. $\gamma_{\text{eff}}^{(m)}$ is the equivalent SNR in an additive white Gaussian noise (AWGN) channel for MCS $m$ that results in the same block error rate (BLER) as the vector channel with SNRs $\gamma_1, \gamma_2, \ldots, \gamma_{N_{\text{sc}}}$. For binary phase shift keying ($\beta_m = 1$) and quadrature phase shift keying ($\beta_m = 2$), the above expression can be derived by equating the BLERs in a vector channel and an AWGN channel [3], [4]. This intuition is then extended to a general MCS by introducing the MCS-dependent parameter $\beta_m$, which is determined empirically to give a good fit. Several studies have validated the accuracy of EESM [3]–[5].

Besides its use in AMC, EESM is a powerful tool that is used for physical layer (PHY) abstraction in OFDM system-level simulations in LTE and WiMAX [6], [7]. It is also used in the real-time operation of cellular systems to generate channel quality indicators (CQIs) [8], which are fed back to the base station (BS) for enabling link adaptation and scheduling.

However, as can be seen from (1), EESM is a non-linear function of the subcarrier SNRs. No exact closed-form expression for its statistics is known. Thus, ad hoc distributions have been used in the literature to approximately characterize its statistics [8], [9]. Another critical issue with EESM is that the scaling parameter $\beta_m$ is quite different for different MCSs [10]. Thus, AMC using EESM involves computing several effective SNRs, one for each MCS, and then selecting the MCS using all of them. Consequently, even EESM-based AMC is more involved than AMC in a narrowband system, and is the focus of this paper.

### A. Contributions

Our objective is to analyze the throughput of EESM-based AMC that is done over a group of frequency-selective subcarriers. To this end, we first present a novel statistical model for EESM, in which the term $\frac{1}{N_{sc}} \sum_{i=1}^{N_{sc}} e^{-\frac{\gamma_i}{\beta_m}}$ inside the logarithm in (1), which lies between 0 and 1, is modeled as a Beta random variable (RV). The choice of the Beta distribution, which has a compact support, is motivated by the central limit approximation for RVs with finite support [11], [12, Chap. 11]. We show that its accuracy is better than that of the lognormal and Gaussian models considered in [8] and [9], respectively, and is comparable to the more involved Pearson and generalized extreme value (GEV) distributions [9], which require evaluating more parameters. Secondly, we derive simple closed-form expressions for the moments of the Beta RV for both independent and correlated subcarriers, and different antenna modes. This is unlike the EESM moments that are required by the lognormal, GEV, and Pearson models, the expressions for which are either very involved or intractable [9].

The proposed model then leads to novel, closed-form expressions for the throughput of AMC in a point-to-point OFDM link. We present an upper bound and an approximation for it, which are verified to be tight. The analysis covers different multiple antenna diversity modes and easily accounts for the correlation among subcarriers.

We then generalize the analysis to cover the multi-cell, multi-user scenario with OFDM. Our model incorporates AMC, rate index feedback, frequency-domain schedulers, multiple antenna diversity, and co-channel interference. Three different schedulers, namely round robin (RR), greedy, and modified proportional fair (MPF) [13], which cover a wide range of the trade-off between user fairness and cell throughput, are analyzed.

### B. Literature on AMC in OFDM

A comprehensive survey of subcarrier-level link adaptation in OFDM, which is also referred to as bit and power loading, is given in [14, Chap. 11]. Instead, we focus on adaptation over a group of subcarriers, which see minor or large variations in channel gains, and is based on LQMs. A generic approach to optimal link adaptation using LQMs subject to a BLER constraint is given in [15], and its throughput with different LQMs has been studied in [1], [15]–[17], but exclusively through simulations. The approaches pursued in [1], [15], [16] can also be considered as providing bounds on the throughput. However, these approaches do not beget analytical expressions for the bounds.

To the best of our knowledge, ours is the first comprehensive analysis of EESM-based AMC in OFDM systems. While [8] considers EESM enabled rate index feedback and frequency-domain scheduling, it does not consider co-channel interference and uses a sub-optimal AMC scheme. A heterogeneous multi-cell orthogonal frequency division multiple access (OFDMA) system with partial feedback and continuous rate adaptation is considered in [18]. However, the channel is assumed to be flat over a resource block, which is the basic feedback and scheduling unit, and its real-valued and continuous signal-to-interference-plus-noise ratio (SINR) is

assumed to be fed back and not the rate. While [19] also considers EESM for cellular network design, its basic model and goal is different from ours, and rate adaptation, feedback, scheduling, and multiple antenna diversity are not modeled.

We note that besides EESM, several other LQMs have been investigated [5], [20]. We focus on EESM because it has a relatively simpler definition than mutual information-based LQMs, in which a piecewise polynomial approximation or numerical integration is required, and is only marginally less accurate by a fraction of a dB [20]. Thus, EESM strikes a good balance between the complexity required to compute it and the accuracy of the BLER estimate obtained from it.

The paper is organized as follows. The point-to-point link system model is described in Section II. A novel statistical model for EESM is developed in Section III. The throughput analysis is presented in Section IV. The multi-cell scenario with scheduling is analyzed in Section V. Our conclusions follow in Section VI.

## II. SYSTEM MODEL: POINT-TO-POINT LINK

We first consider a point-to-point OFDM link where the transmitted codeword is encoded across $N_{sc}$ subcarriers. The receiver selects an MCS based on the SNRs of these subcarriers and feeds it back to the transmitter using a feedback channel. The feedback is assumed to be error-free and the feedback delay is assumed to be negligible [1], [8], [10], [16], [18]. The transmitter then uses the reported MCS for transmission.

Let $h_i(k,l)$ denote the complex baseband channel gain between the $l^{th}$ transmit antenna and the $k^{th}$ receive antenna of the $i^{th}$ subcarrier. The complex channel gains are identically distributed and are circularly symmetric complex Gaussian RVs with unit variance, which models Rayleigh fading [2]. The channel gains between different transmit-receive (Tx-Rx) antenna pairs are assumed to be independent, i.e., $h_i(k,l)$ is independent of $h_j(m,n)$ if $k \neq m$ or $l \neq n$, for any $i$ and $j$, which is valid when the antennas are sufficiently spaced apart in a rich scattering environment. Let $\mathbf{H}_i$ denote the $N_r \times N_t$ channel matrix of the $i^{th}$ subcarrier with $h_i(k,l)$ as the $(k,l)^{th}$ element. Here, $N_r$ and $N_t$ denote the number of receive and transmit antennas, respectively.

Let $\sigma^2$ denote the average SNR of a Tx-Rx link and $\gamma_i$ denote the SNR of the $i^{th}$ subcarrier, for $1 \leq i \leq N_{sc}$. For single-input-single-output (SISO) with $N_t = N_r = 1$, $\gamma_i = \sigma^2 |h_i(1,1)|^2$. For single-input-multiple-output (SIMO) with $N_t = 1$, $N_r > 1$, and maximal ratio combining (MRC), $\gamma_i = \sigma^2 \sum_{k=1}^{N_r} |h_i(k,1)|^2$. Similarly, for closed-loop multiple-input-single-output (MISO) with $N_t > 1$, $N_r = 1$, and maximal ratio transmission (MRT), $\gamma_i = \sigma^2 \sum_{l=1}^{N_t} |h_i(1,l)|^2$. For single stream $N_r \times N_t$ multiple-imput-multiple-output (MIMO) diversity transmission, $\gamma_i = \sigma^2 \lambda_i^2$, where $\lambda_i$ is the largest singular value of the matrix $\mathbf{H}_i$. Let $\mathbf{\Gamma} = [\gamma_1, \gamma_2, \ldots, \gamma_{N_{sc}}]$ denote the vector of subcarrier SNRs.

Let $\Omega$ denote the set of $L$ MCSs used for AMC. The information rate of MCS $m$ is denoted by $r_m$ and the MCSs are indexed in the increasing order of their rates, i.e., $r_1 \leq r_2 \leq \cdots \leq r_L$. The effective SNR for MCS $m$ is denoted by $\gamma_{eff}^{(m)}$ and the corresponding MCS-dependent

scaling parameter by $\beta_m$. Let $m_{\text{opt}}$ denote the selected MCS and let $\text{BLER}_t$ denote the maximum allowable block error rate. $\text{BLER}(\mathbf{\Gamma}, m)$ denotes the BLER of MCS $m$ when it is transmitted over $N_{\text{sc}}$ subcarriers whose SNRs are given by $\mathbf{\Gamma}$.

### A. Optimal AMC Using EESM

In order to maximize the average throughput, the optimal MCS is chosen as a function of $\mathbf{\Gamma}$ as follows:

$$\underset{m \in \Omega}{\arg \max} \; r_m, \qquad (2)$$

$$\text{s. t. } \text{BLER}(\mathbf{\Gamma}, m) \leq \text{BLER}_t. \qquad (3)$$

By the definition of EESM, we have

$$\text{BLER}(\mathbf{\Gamma}, m) \approx \text{BLER}_{\text{AWGN}}\left(\gamma_{\text{eff}}^{(m)}, m\right), \qquad (4)$$

where $\text{BLER}_{\text{AWGN}}(\cdot, m)$ denotes the BLER in an AWGN channel for MCS $m$. This is an approximation and not an equality because EESM can occasionally predict an incorrect BLER. Such errors are inherent in all LQMs because they map $N_{\text{sc}}$ gains into a single number. This error probability is among the lowest for EESM [3], [5], [15]. For tractability, we assume it to be negligible. Therefore, this approximation is assumed to be exact henceforth.

Thus, using EESM, the BLER constraint in (3) can be mapped to a constraint on the effective SNR as follows. Let $T_m$ denote the lowest SNR at which the BLER in the AWGN channel using MCS $m$ is $\text{BLER}_t$:

$$\text{BLER}_{\text{AWGN}}(T_m, m) = \text{BLER}_t, \quad m = 1, \dots, L. \qquad (5)$$

Thus, the BLER constraint is equivalent to requiring that the effective SNR of MCS $m$ be greater than or equal to $T_m$. Since the BLER in an AWGN channel is a continuous and strictly decreasing function of the SNR, the intermediate value theorem guarantees a unique solution for $T_m$.

The optimal AMC scheme is now driven by the thresholds $T_1, T_2, \dots, T_L$, and proceeds as follows. It chooses the highest rate MCS if its effective SNR is greater than or equal to $T_L$, i.e., $\gamma_{\text{eff}}^{(L)} \geq T_L$. Else, the scheme moves to the next highest MCS, and so on. If $\gamma_{\text{eff}}^{(i)} < T_i$, for all $i = 1, \dots, L$, then no data transmission takes place and is indexed by MCS 0. Here, the subcarrier SNRs are so low that the BLER of all the MCSs exceeds $\text{BLER}_t$. Note that given the sequential nature of the search, no tie between different MCSs occurs.

*Note:* An alternate AMC formulation is to maximize the goodput [21]. A sufficient condition for the two formulations to be equivalent is: $\text{BLER}_t \leq \underset{m_1, m_2 \in \Omega}{\min}\left\{1 - \frac{r_{m_1}}{r_{m_2}}\right\}$, where $r_{m_1} < r_{m_2}$ [16]. Further, if the BLER waterfall curves in an AWGN channel can be approximated by a step function, then again the two formulations are equivalent.

### B. Notations

Let $\mathbf{I}_n$ and $\mathbf{0}_n$ denote the $n \times n$ identity matrix and zero matrix, respectively. The determinant of a matrix $\mathbf{A}$ is denoted by $\det(\mathbf{A})$ and its transpose by $\mathbf{A}^T$. The matrix $\text{diag}(\mathbf{v})$ denotes a diagonal matrix with elements of the vector $\mathbf{v}$ as its diagonal elements. Let $\left[0, \dots, 0, \underset{(i)}{s}, 0, \dots, 0\right]$ denote a vector whose $i^{\text{th}}$ element is $s$ and all other elements are 0. Let $\text{Re}(c)$, $\text{Im}(c)$, and $c^*$ respectively denote the real part, the imaginary part, and the complex conjugate of the complex number $c$. Let $\mathbb{E}[X]$ and $\text{var}(X)$ denote the expectation and variance of the RV $X$, respectively.

### III. STATISTICAL MODEL FOR EESM

In order to analyze the performance of EESM-based AMC, a statistical model for EESM is required. Since no closed-form expression for the distribution of EESM is available owing to its non-linear nature, we first present a novel and tractable approximation for it.

Let $Y_m = \frac{1}{N_{\text{sc}}} \sum_{i=1}^{N_{\text{sc}}} e^{-\frac{\gamma_i}{\beta_m}}$. Notice that $e^{-\frac{\gamma_i}{\beta_m}} \in [0, 1]$. Thus, $Y_m \in [0, 1]$ is an average of $N_{\text{sc}}$ positive RVs with finite support. For independent subcarriers, the strong law of large numbers suggests that $Y_m$ is a constant. However, for values of $N_{\text{sc}}$ that are of practical interest, this turns out to be inadequate. Another approach, which is motivated by the central limit theorem, is to approximate $Y_m$ scaled by $\sqrt{N_{\text{sc}}}$ as a Gaussian RV [9]. However, $Y_m \in [0, 1]$, while a Gaussian RV has a support of $(-\infty, \infty)$; as we shall see, the Gaussian model is quite inaccurate.

We propose a new statistical model for EESM that is motivated by the central limit approximation, in which the sum of i.i.d. RVs with finite support is approximated by a Beta distribution [12, Chap. 11]. Thus, we model the RV $Y_m = \frac{1}{N_{\text{sc}}} \sum_{i=1}^{N_{\text{sc}}} e^{-\frac{\gamma_i}{\beta_m}}$ as a Beta RV.

Let $Z_m$ denote a Beta distributed RV with parameters $a_m$ and $b_m$. Then, its probability density function (PDF) is given by

$$f_{Z_m}(z) = \frac{z^{(a_m - 1)}(1 - z)^{(b_m - 1)}}{B(a_m, b_m)}, \quad 0 \leq z \leq 1, \qquad (6)$$

where $B(\cdot, \cdot)$ is the Beta function and its cumulative distribution function (CDF) is given by $F_{Z_m}(z) = B_i(z, a_m, b_m)$, $0 \leq z \leq 1$, where $B_i(\cdot, \cdot, \cdot)$ is the incomplete Beta function [22]. The parameters $a_m$ and $b_m$ can be expressed in terms of the mean and variance of $Z_m$ as

$$a_m = \frac{\mathbb{E}[Z_m]\left(\mathbb{E}[Z_m] - \mathbb{E}[Z_m]^2 - \text{var}(Z_m)\right)}{\text{var}(Z_m)}, \qquad (7)$$

$$b_m = \frac{(1 - \mathbb{E}[Z_m])\left(\mathbb{E}[Z_m] - \mathbb{E}[Z_m]^2 - \text{var}(Z_m)\right)}{\text{var}(Z_m)}. \qquad (8)$$

The moment-matching method matches $\mathbb{E}[Z_m]$ and $\text{var}(Z_m)$ with the mean $\mu_m$ and variance $v_m$ of $Y_m$ in order to determine $a_m$ and $b_m$. From (1), the CDF of $\gamma_{\text{eff}}^{(m)}$, denoted by $F_{\gamma_{\text{eff}}^{(m)}}(x)$, can be written in terms of the PDF of $Y_m$ as $P\left(Y_m \geq e^{-\frac{x}{\beta_m}}\right)$. Using the proposed Beta approximation for $Y_m$, it is approximately given by

$$F_{\gamma_{\text{eff}}^{(m)}}(x) \approx 1 - B_i\left(e^{-\frac{x}{\beta_m}}, a_m, b_m\right), \quad x \geq 0. \qquad (9)$$

Notice that we approximate the term inside the logarithm as a Beta RV. Our approach differs from the approaches used in [8], [9], which attempt to directly approximate the distribution of EESM itself. A key advantage of our approach is that it enables a closed-form computation of the moments,

as we shall see next. It is unlike the lognormal, Pearson, and GEV distributions that use EESM moments, the analytical expressions for which are either very involved or intractable [9].

### A. Closed-form Expressions for the Mean and Variance of $Y_m$

We see from (7) and (8) that the Beta distribution is fully specified in terms of its mean and variance. We now derive closed-form expressions for these for different antenna modes. We consider the cases where the subcarrier SNRs are independent and when they are correlated. The former scenario is simpler and insightful, and occurs when the subcarrier bandwidth is close to the coherence bandwidth of the channel. It also arises if the subcarriers are noncontiguous, as in the full usage of subchannels (FUSC) or partial usage of subchannels (PUSC) modes of WiMAX. Otherwise, the subcarrier SNRs are correlated. This scenario often occurs in LTE and in the Band AMC mode of WiMAX, in which contiguous subcarriers are allotted to a user.

*1) Independent Subcarriers:* We first state the following general result.

**Result 1:** The mean and variance of $Y_m$, when each subcarrier SNR $\gamma_i$ is a Chi-square RV with $\tau$ degrees of freedom and mean $c\tau$, are given by

$$\mu_m = \left(1 + 2c\beta_m^{-1}\right)^{-\frac{\tau}{2}}, \tag{10}$$

$$v_m = \frac{1}{N_{sc}} \left[ \left(1 + 4c\beta_m^{-1}\right)^{-\frac{\tau}{2}} - \left(1 + 2c\beta_m^{-1}\right)^{-\tau} \right]. \tag{11}$$

*Proof:* The proof is relegated to Appendix A. ∎

The mean and variance of the RV $Y_m$ depend on the antenna mode through $c$ and $\tau$, and can be evaluated as follows. For SISO, $c = \frac{\sigma^2}{2}$ and $\tau = 2$. For SIMO with MRC, $c = \frac{\sigma^2}{2}$ and $\tau = 2N_r$. Similarly, for MISO with MRT, $c = \frac{\sigma^2}{2}$ and $\tau = 2N_t$. For MISO with the Alamouti space-time code, $c = \frac{\sigma^2}{4}$ and $\tau = 4$ [2]. For single stream MIMO, $\gamma_i$ is the square of the largest singular value of the matrix $\mathbf{H}_i$, and is not a Chi-square RV. We state the result for $2 \times 2$ MIMO here.[1]

**Result 2:** The mean and variance of the RV $Y_m$ for single stream $2 \times 2$ MIMO are given by

$$\mu_m = \frac{2\beta_m \left(\beta_m^2 + \sigma^4 + \beta_m\sigma^2\right)}{\left(\beta_m + \sigma^2\right)^3} - \frac{2\beta_m}{2\beta_m + \sigma^2}, \tag{12}$$

$$v_m = \frac{1}{N_{sc}} \left[ \frac{2\beta_m \left(\beta_m^2 + 4\sigma^4 + 2\beta_m\sigma^2\right)}{\left(\beta_m + 2\sigma^2\right)^3} - \frac{\beta_m}{\beta_m + \sigma^2} - \mu_m^2 \right]. \tag{13}$$

*Proof:* The proof is relegated to Appendix B. ∎

*2) Correlated Subcarriers:* In this scenario, the channel gains of any two subcarriers for the same transmit-receive antenna pair are correlated. In general, the channel gain vector $\mathbf{h}_{kl} = [h_1(k,l), \ldots, h_{N_{sc}}(k,l)]^T$ is modeled as a circularly symmetric complex Gaussian random vector with covariance matrix $\mathbf{C}$, whose $(i,j)^{th}$ element is given by $C_{ij} = \mathbb{E}\left[h_i(k,l)h_j(k,l)^*\right]$.

We state the following general result.

---

[1]The moment generating function (MGF) of $\gamma_i$ for the general case is derived in [23]. Then, the mean and variance of $Y_m$ can be obtained using (28) and (29), respectively, in Appendix A. We do not state the results here as they are quite involved.

**Result 3:** The mean and variance of $Y_m$ with correlated subcarriers, for SISO ($N_t = N_r = 1$), MISO ($N_t > 1, N_r = 1$), and SIMO ($N_t = 1, N_r > 1$) are given by

$$\mu_m = \det\left(\mathbf{I}_{2N_{sc}} - 2\sigma^2\mathbf{K}\mathbf{P}^{(m)}\right)^{-\frac{\max(N_t, N_r)}{2}}, \tag{14}$$

$$v_m = \frac{1}{N_{sc}^2} \sum_{i=1}^{N_{sc}} \sum_{j=1}^{N_{sc}} \det\left(\mathbf{I}_{2N_{sc}} - 2\sigma^2\mathbf{K}\mathbf{Q}_{ij}^{(m)}\right)^{-\frac{\max(N_t, N_r)}{2}} - \mu_m^2, \tag{15}$$

where $\mathbf{P}^{(m)} = \begin{bmatrix} \mathbf{R}^{(m)} & \mathbf{0}_{N_{sc}} \\ \mathbf{0}_{N_{sc}} & \mathbf{R}^{(m)} \end{bmatrix}$, $\mathbf{Q}_{ij}^{(m)} = \begin{bmatrix} \mathbf{S}_{ij}^{(m)} & \mathbf{0}_{N_{sc}} \\ \mathbf{0}_{N_{sc}} & \mathbf{S}_{ij}^{(m)} \end{bmatrix}$,

$\mathbf{R}^{(m)} = \mathrm{diag}\left([-\beta_m^{-1}, 0, \ldots, 0]\right)$, $\mathbf{K} = \frac{1}{2}\begin{bmatrix} \mathrm{Re}(\mathbf{C}) & -\mathrm{Im}(\mathbf{C}) \\ \mathrm{Im}(\mathbf{C}) & \mathrm{Re}(\mathbf{C}) \end{bmatrix}$,

$$\mathbf{S}_{ij}^{(m)} = \mathrm{diag}\left(\left[0, \ldots, 0, \underset{(i)}{-\beta_m^{-1}}, 0, \ldots, 0, \underset{(j)}{-\beta_m^{-1}}, 0, \ldots, 0\right]\right),$$

for $i \neq j$, and $\mathbf{S}_{ii}^{(m)} = \mathrm{diag}\left(\left[0, \ldots, 0, \underset{(i)}{-2\beta_m^{-1}}, 0, \ldots, 0\right]\right)$.

*Proof:* The proof is relegated to Appendix C. ∎

MISO with the Alamouti space-time code is equivalent to closed-loop MISO with half the transmit power [2]. Therefore, the mean and variance expressions for the Alamouti space-time code follow from (14) and (15), with $\mathbf{K}$ replaced by $\frac{\mathbf{K}}{2}$.

For single stream $N_r \times N_t$ MIMO, no result on the joint distribution of correlated singular values is available to the best of our knowledge when the component channel gains are correlated. Therefore, we use the Monte Carlo method to find the mean and variance [24]. In it, empirical moments are used to approximate actual moments. The key advantage of this method is that the approximation error decreases as $\mathcal{O}(\sqrt{W})$, where $W$ is the sample size [24]. It has also been extensively used elsewhere in the literature [8], [25]. In our problem, $W$ samples of the channel matrix $\mathbf{H}_i$ with the required correlation across the subcarriers are generated. From these, $W$ samples of the largest singular value are obtained, and are then used to compute the empirical moments of $Y_m$. Note that this is a one-time task, and the same samples can be used for finding in parallel the moments of $Y_m$ for different MCSs.

### B. Error Analysis of the Beta Approximation

We now derive an expression for the error in the Beta approximation as an infinite series in terms of the higher order moments of $Y_m$. First, we define an alternative form of the Jacobi polynomial as [26]

$$G_n(a_m, b_m, x) = n! \frac{\Gamma(n + a_m + b_m - 1)}{\Gamma(2n + a_m + b_m - 1)} \times J_n(b_m - 1, a_m - 1, 2x - 1), \quad 0 < x < 1, \tag{16}$$

where $\Gamma(\cdot)$ is the Gamma function and $J_n(a, b, \cdot)$ is the standard Jacobi polynomial of order $n$ with parameters $a$ and $b$ [22]. Then, the approximation error $\epsilon(x) = f_{Y_m}(x) - f_{Z_m}(x)$, as shown in Appendix D, is given by

$$\epsilon(x) = f_{Z_m}(x) \sum_{k=1}^{\infty} c_k G_k(a_m, b_m, x), \tag{17}$$

where $c_k = \frac{(2k + a_m + b_m - 1)\Gamma(2k + a_m + b_m - 1)^2 B(a_m, b_m)}{k!\Gamma(k + a_m)\Gamma(k + a_m + b_m - 1)\Gamma(k + b_m)}$ $\times \mathbb{E}\left[G_k(a_m, b_m, Y_m)\right]$. Note that $G_k(a_m, b_m, x)$ is a $k^{th}$

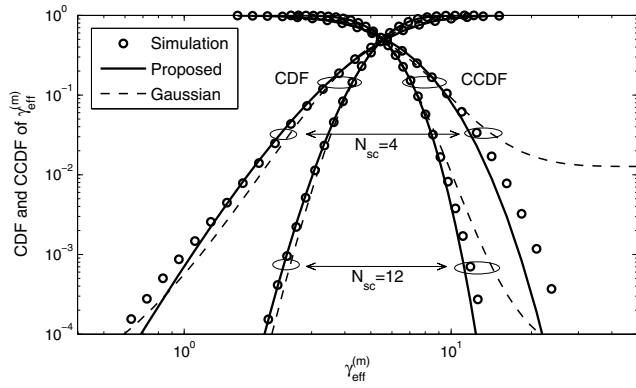Fig. 1. Comparison of CDF and CCDF of EESM with the proposed Beta distribution-based model for different numbers of independent subcarriers ($\sigma^2 = 10$ dB, $\beta_m = 5$, and $\tau = 2$).

order polynomial. Hence, the higher order moments of $Y_m$ required to evaluate $\mathbb{E}\left[G_k(a_m, b_m, Y_m)\right]$ can be obtained from the MGF results in Appendix A for independent subcarriers, and in Appendix C for correlated subcarriers.

### C. Empirical Verification of the Proposed Beta Model

In order to assess the accuracy, we compare the CDF and complementary CDF (CCDF) of the proposed distribution approximation with the empirical CDF and CCDF, as has also been done in other wireless modeling problems [8], [27], [28]. The CDF captures the accuracy of the fit for low values of $\gamma_{\text{eff}}^{(m)}$. However, it saturates to 1 for large $\gamma_{\text{eff}}^{(m)}$ values for any distribution. In this regime, comparing the CCDF is more instructive. An alternate way to assess the accuracy is using Kullback-Leibler (KL) divergence; the smaller its value, the better the accuracy. The KL divergences for the proposed Beta model, Gaussian, lognormal, GEV, and Pearson are $16 \times 10^{-4}, 43 \times 10^{-4}, 22 \times 10^{-4}, 18 \times 10^{-4}, 7 \times 10^{-4}$, respectively, for $N_{\text{sc}} = 12$, and $8 \times 10^{-4}, 21 \times 10^{-4}, 11 \times 10^{-4}, 35 \times 10^{-4}, 5 \times 10^{-4}$ for $N_{\text{sc}} = 24$, respectively, for independent subcarriers. Notice that the KL divergence for the proposed Beta distribution is less than the Gaussian, lognormal, and GEV distributions and is comparable to the Pearson distribution. Further, it decreases as $N_{\text{sc}}$ increases.[2]

*1) Independent Subcarriers:* Figure 1 compares the empirical CDF and CCDF with those for the proposed Beta, and Gaussian models, for $\tau = 2$ (SISO). We observe that the Beta model is quite accurate up to three orders of magnitude even for $N_{\text{sc}} = 4$. Its accuracy improves as $N_{\text{sc}}$ increases. It works better than the Gaussian model. Further, the Gaussian CCDF saturates for high values of $\gamma_{\text{eff}}^{(m)}$, which correspond to small values of $Y_m$, as it assigns a non-zero probability to negative values, which $Y_m$ cannot take.

Figure 2 compares the CDFs of the different approximations. A zoomed-in plot is shown in order to make the curves discernible. The parameters for the GEV, Pearson, and lognormal distributions are obtained by moment-matching, and the

[2]We have observed that none of the distributions proposed in the literature, including ours, pass the goodness-of-fit tests such as Kolmogorov-Smirnov (KS) and Chi-square tests [29]. We, therefore, do not compare the distributions on the basis of these tests.
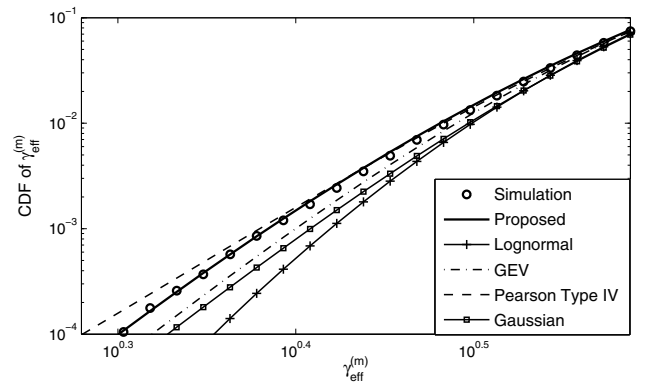


Fig. 2. Comparison of CDFs of the different approximations with the empirical CDF of EESM for independent subcarriers ($\sigma^2 = 10$ dB, $\beta_m = 5$, and $N_{\text{sc}} = 12$).
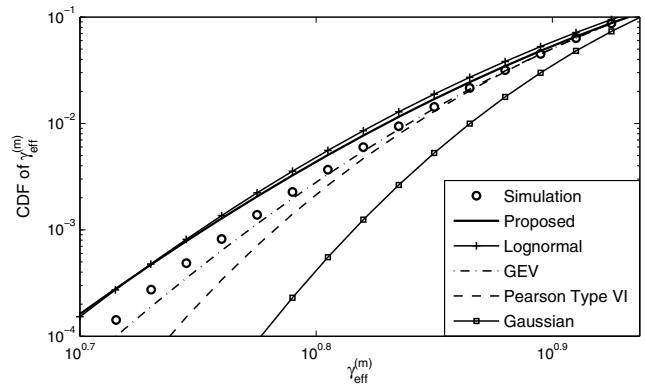


Fig. 3. Comparison of CDFs of the different approximations with the empirical CDF of EESM for geometrically correlated subcarriers ($\sigma^2 = 10$ dB, $\beta_m = 5$, $N_{\text{sc}} = 12$, and $\rho = 0.4$).

moments are obtained by the Monte Carlo method [24]. We see that the proposed Beta model, despite its simpler form, is as accurate as the GEV and Pearson distributions, and is more accurate than the lognormal and Gaussian models. The accuracy in matching the CCDF is similar.

*2) Correlated Subcarriers:* In order to study the effect of correlation, we set $C_{ij} = \rho^{|i-j|}$, for $0 < \rho < 1$ [8]. Thus, $\rho$ close to 1 implies highly correlated subcarriers, while $\rho$ close to 0 implies uncorrelated subcarriers. Figure 3 compares the CDFs of the different models for $\rho = 0.4$ and $\tau = 4$ ($1 \times 2$ SIMO). The proposed model tracks the empirical CDF well, and its accuracy is again comparable to the more involved GEV and Pearson distributions.

## IV. THROUGHPUT ANALYSIS USING BETA MODEL

We now analyze the throughput of the optimal AMC scheme described in Section II-A. The average throughput $\overline{R}$ equals

$$\overline{R} = \sum_{m=1}^{L} r_m \Pr\{m_{\text{opt}} = m\}. \tag{18}$$

The AMC scheme chooses MCS $m$ if its effective SNR exceeds $T_m$, and the effective SNRs for the higher rate MCSs

are below their corresponding thresholds. Thus,

$$\Pr\{m_{\text{opt}} = m\} = P\left(\gamma_{\text{eff}}^{(m)} \geq T_m, \gamma_{\text{eff}}^{(m+1)} < T_{m+1}, \dots, \right.$$
$$\left. \gamma_{\text{eff}}^{(L)} < T_L\right). \quad (19)$$

Hence, to compute (19), the $(L - m + 1)$-dimensional joint distribution of the effective SNRs $\left\{\gamma_{\text{eff}}^{(m)}, \gamma_{\text{eff}}^{(m+1)}, \dots, \gamma_{\text{eff}}^{(L)}\right\}$ is needed. However, even with independent subcarriers, the effective SNRs of different MCSs are correlated, since they are obtained from the same vector $\boldsymbol{\Gamma}$, but with different $\beta_m$. No closed-form result is available for their joint distribution. We circumvent this problem by coming up with a novel upper bound and an approximation. Before stating the final results, we state the following lemma, which we shall refer to as the *ordering property* of EESM.

**Lemma** *1:* $\gamma_{\text{eff}} = -\beta \ln\left(\frac{1}{N_{\text{sc}}} \sum_{i=1}^{N_{\text{sc}}} e^{-\frac{\gamma_i}{\beta}}\right)$ is an increasing function of $\beta$, except when $\gamma_1 = \gamma_2 = \dots = \gamma_{N_{\text{sc}}} = \gamma$, in which case $\gamma_{\text{eff}} = \gamma$ and $\gamma_{\text{eff}}$ is not a function of $\beta$.

*Proof:* The proof is relegated to Appendix E. ∎

The MCSs used for WiMAX along with the $\beta_m$ parameters and SNR thresholds are given in Table I. The corresponding parameters for LTE are given in [10, Tbl. I]. In both tables, we see that as $r_m$ increases, $\beta_m$ also increases. Thus, for every $\boldsymbol{\Gamma}$, the EESM is larger for a higher rate MCS.

**Result** *4:* The average throughput is upper bounded as follows:

$$\overline{R} \leq \sum_{m=1}^{L-1} r_m \min\left\{B_i\left(e^{-\frac{T_m}{\beta_m}}, a_m, b_m\right)\right.$$
$$- B_i\left(e^{-\frac{T_{m+1}}{\beta_m}}, a_m, b_m\right), B_i\left(e^{-\frac{T_m}{\beta_{m+1}}}, a_{m+1}, b_{m+1}\right)$$
$$\left. - B_i\left(e^{-\frac{T_{m+1}}{\beta_{m+1}}}, a_{m+1}, b_{m+1}\right)\right\} + r_L B_i\left(e^{-\frac{T_L}{\beta_L}}, a_L, b_L\right).$$
$$(20)$$

Furthermore, $\overline{R}$ is approximately given by

$$\overline{R} \approx r_L B_i\left(e^{-\frac{T_L}{\beta_L}}, a_L, b_L\right) + \sum_{m=1}^{L-1} r_m \left[B_i\left(e^{-\frac{T_m}{\beta_m}}, a_m, b_m\right)\right.$$
$$\left. - B_i\left(e^{-\frac{T_{m+1}}{\beta_{m+1}}}, a_{m+1}, b_{m+1}\right)\right]. \quad (21)$$

*Proof:* The derivation is relegated to Appendix F. ∎
Note that both the upper bound and the approximation only require the marginal distribution of EESM. Hence, they can be readily computed using the results in Section III.

### A. Numerical Results

We now compare the analytical results with numerical simulations. The maximum allowable block error rate $\text{BLER}_t$ is 0.1 [30]. Results are shown for both LTE and WiMAX, which use different sets of MCSs. The number of subcarriers $N_{\text{sc}}$ is 24, which is equal to two physical resource blocks (PRBs) in LTE or three bins in the Band AMC mode of WiMAX (ignoring the pilot subcarriers). For SIMO, we use $N_r = 2$, for MISO, we use $N_t = 2$, and for MIMO, we use $N_r = N_t = 2$. We consider the typical urban (TU) channel,

TABLE I
$\beta_m$ VALUES AND SNR THRESHOLDS FOR MCSs SPECIFIED IN THE
WiMAX STANDARD (BLER$_t$ = 0.1)

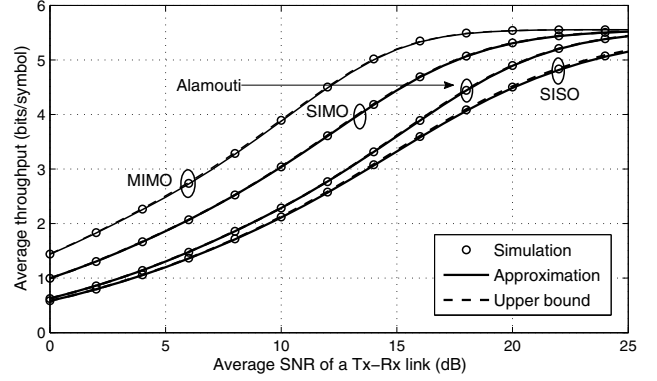| Index ($m$) | Modulation | Code rate | Information rate $r_m$ (bits/symbol) | $\beta_m$ | SNR threshold (dB) |
|---|---|---|---|---|---|
| 1 | QPSK | 1/2 | 1.00 | 1.66 | 1.65 |
| 2 | QPSK | 3/4 | 1.50 | 1.75 | 4.77 |
| 3 | 16-QAM | 1/2 | 2.00 | 9.58 | 8.40 |
| 4 | 16-QAM | 3/4 | 3.00 | 9.60 | 11.54 |
| 5 | 64-QAM | 2/3 | 4.00 | 40.50 | 16.79 |
| 6 | 64-QAM | 3/4 | 4.50 | 41.00 | 17.51 |
| 7 | 64-QAM | 5/6 | 5.00 | 41.50 | 18.89 |



Fig. 4. LTE: Average throughput versus average SNR of a transmit-receive antenna pair link ($\sigma^2$) for the RA channel ($N_{\text{sc}} = 24$, $\text{BLER}_t = 0.1$, BW = 5 MHz, and 512-point FFT).

whose root mean square (RMS) delay spread is 0.5 $\mu$s, and the less-dispersive rural area (RA) channel, whose RMS delay spread is 0.1 $\mu$s [31]. We use a 512-point FFT and the bandwidth is 5 MHz. The sampling frequencies for LTE and WiMAX are 7.68 MHz [6] and 5.6 MHz [7], respectively.

The throughput as a function of $\sigma^2$ for different antenna diversity modes for LTE is plotted in Figures 4 and 5 for the RA and TU channels, respectively. For WiMAX, the corresponding plot for the TU channel is shown in Figure 6. Notice the excellent match between the approximation and the simulation curves for all the antenna modes for both LTE and WiMAX. Further, the upper bound is reasonably tight in all the plots and becomes tighter as we go from SISO to MIMO. The key step in deriving the analytical expressions for the throughput is to upper bound (19) with $P\left(\gamma_{\text{eff}}^{(m)} \geq T_m, \gamma_{\text{eff}}^{(m+1)} < T_{m+1}\right)$ (cf. (35)). Notice that this bivariate upper bound is exact for a narrowband fading channel, where the subcarrier SNRs are all equal. This also explains why the upper bound is tighter in the less-dispersive RA channel plots in Figure 4 than in the TU channel plots in Figure 5. In a wideband channel, however, one cannot guarantee the exactness of this upper bound. However, one expects it to be exact for most subcarrier gain realizations because it is unlikely that a higher rate MCS is feasible when a lower rate MCS is not. For example, in our simulations this happened in less than $0.005\%$ of the channel realizations.

The throughput as a function of $N_{\text{sc}}$ for different antenna modes for the RA channel, TU channel, and uncorrelated subcarriers is plotted in Figure 7. Plots for the Alamouti space-time code are skipped to avoid clutter. The throughput
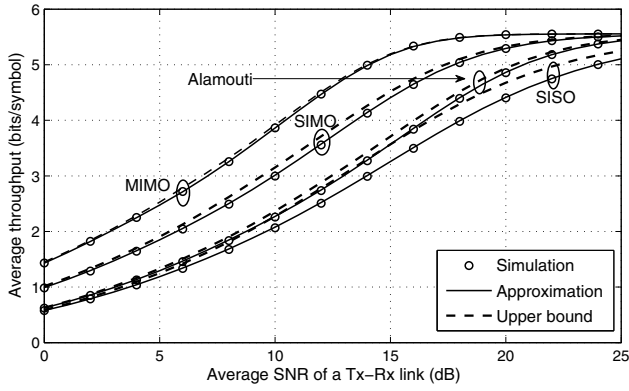
Fig. 5. LTE: Average throughput versus average SNR of a transmit-receive antenna pair link ($\sigma^2$) for the TU channel ($N_{sc} = 24$, $BLER_t = 0.1$, $BW = 5$ MHz, and 512-point FFT).
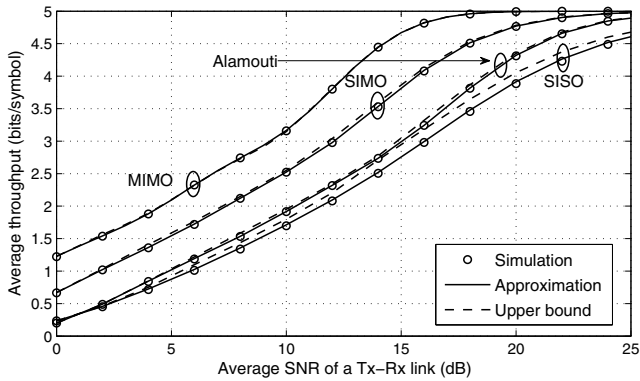


Fig. 6. WiMAX: Average throughput versus average SNR of a transmit-receive antenna pair link ($\sigma^2$) for the TU channel ($N_{sc} = 24$, $BLER_t = 0.1$, $BW = 5$ MHz, and 512-point FFT).

for SISO and SIMO decreases marginally as the number of subcarriers increases. While the same behavior is observed for single-stream MIMO for the TU and RA channels, its throughput marginally increases as $N_{sc}$ increases for uncorrelated subcarriers.

## V. AMC IN MULTI-CELL, MULTI-USER SCENARIO WITH SCHEDULING

We now analyze the downlink cell throughput of a multi-cell system with co-channel interferers and frequency-domain scheduling. As before, a codeword is encoded across $N_{sc}$ subcarriers. However, multiple users now contend for the same $N_{sc}$ subcarriers. Hence, a frequency-domain scheduler is used at the BS to select the appropriate user. Based on the channel power gains of the $N_{sc}$ subcarriers, each user feeds back to the BS the index of the highest rate MCS it can receive whose BLER is below $BLER_t$. The feedback is error-free and the feedback delay is negligible. Full frequency reuse is assumed.

We consider a cell with $K$ users and $M$ neighboring BSs. A BS transmits with power $P_S$. Let $x_0^{(n)}$ denote the data sent by the serving BS 0, $x_j^{(n)}$ denote the data received from the $j^{th}$ BS on the $n^{th}$ subcarrier, and let $\sqrt{\alpha_{0k}}h_{0k}^{(n)}(l)$ and $\sqrt{\alpha_{jk}}h_{jk}^{(n)}(l)$ denote the corresponding complex channel gains for the $l^{th}$ receive antenna. The small-scale fading term $h_{jk}^{(n)}(l)$ is a circularly symmetric complex Gaussian RV with
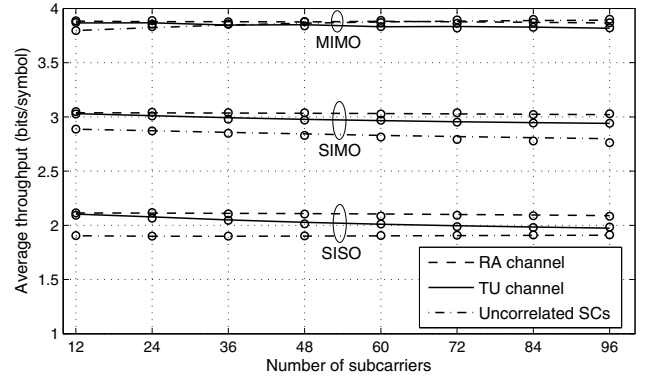
unit variance, which models Rayleigh fading. The lognormal RV $\alpha_{jk}$ models shadowing. Thus, $\alpha_{jk}$ expressed in dB is a Gaussian RV with mean $-L_0 - 10\eta \log\left(\frac{d_{jk}}{d_0}\right)$ and standard deviation $\sigma_{shad}$, where $L_0$ is the pathloss in dB at a reference distance $d_0$ from the BS, $d_{jk}$ is the distance between user $k$ and BS $j$, and $\eta$ is the pathloss exponent. Without loss of generality, the average powers of $x_0^{(n)}$ and $x_j^{(n)}$ are normalized to unity, and $z_k^{(n)}(l)$ denotes white Gaussian noise with power $P_N$. Then, the received signal for the scheduled user $k$ on the $n^{th}$ subcarrier and the $l^{th}$ receive antenna is given by

$$y_k^{(n)}(l) = \sqrt{P_S}\sqrt{\alpha_{0k}}h_{0k}^{(n)}(l)x_0^{(n)} + \sqrt{P_S}\sum_{j=1}^{M}\sqrt{\alpha_{jk}}h_{jk}^{(n)}(l)x_j^{(n)} + z_k^{(n)}(l), \quad l = 1, \ldots, N_r. \quad (22)$$

The complex channel gains of different receive antennas $h_{jk}^{(n)}(1), \ldots, h_{jk}^{(n)}(N_r)$ are assumed to be independent, which is valid if the receive antennas are sufficiently spaced apart in a rich scattering environment [2]. The received SINR with MRC for the $k^{th}$ user on the $n^{th}$ subcarrier $\gamma_k^{(n)}$ is given by

$$\gamma_k^{(n)} = $$

$$\frac{P_S\alpha_{0k}\left(\sum_{l=1}^{N_r}\left|h_{0k}^{(n)}(l)\right|^2\right)^2}{P_S\sum_{j=1}^{M}\alpha_{jk}\left|\sum_{l=1}^{N_r}h_{0k}^{(n)}(l)^*h_{jk}^{(n)}(l)\right|^2 + P_N\sum_{l=1}^{N_r}\left|h_{0k}^{(n)}(l)\right|^2}. \quad (23)$$

The analysis can be extended to the MISO and MIMO antenna diversity modes using the corresponding SINR expressions.

We consider the following schedulers, which cover a wide range of the fairness versus throughput trade-off:

a) *Greedy Scheduler:* It selects the user that reports the highest rate. In case multiple users report the same highest rate, one of them is chosen with equal probability. While the greedy scheduler maximizes the throughput, it is unfair because users closer to the BS get scheduled more often.

b) *RR Scheduler:* It selects users in a pre-determined periodic manner. Each user is scheduled once within a period, making the scheduler time-fair. However, it does not exploit mult-user diversity.

c) *MPF Scheduler:* It chooses the user that has the maximum MPF metric, which is defined as the ratio of the rate reported by the user to its fading-averaged value [13]. It has been used in the literature for tractability [8], [13], [32]. It achieves a compromise between maximizing the cell throughput and ensuring user fairness, which is similar to the PF scheduler [33].

### A. Cell Throughput Analysis

*1) Beta Model for EESM:* As before, we model $Y_{m,k} = \frac{1}{N_{sc}} \sum_{n=1}^{N_{sc}} e^{-\frac{\gamma_k^{(n)}}{\beta_m}}$ as a Beta RV whose parameters are denoted by $a_{m,k}$ and $b_{m,k}$. With co-channel interference, the joint distribution of $\left\{ \gamma_k^{(1)}, \gamma_k^{(2)}, \ldots, \gamma_k^{(N_{sc})} \right\}$ is not known. Hence, it is no longer possible to derive closed-form expressions for the moments of $Y_{m,k}$. Therefore, we use the aforementioned Monte Carlo method to compute its moments. Note that the Monte Carlo method only involves generating samples of $Y_{m,k}$, while a full system simulation further involves simulating AMC, feedback of the MCS index, scheduler, and transmission to the scheduled user with the reported MCS. Thus, a full system simulation is more computationally intensive and time consuming. As discussed in Section III-A2, the approximation error in the Monte Carlo method decays as $\mathcal{O}(\sqrt{W})$, where $W$ is the sample size [24].

*2) Cell Throughput:* Let $C_k$ denote the throughput of user $k$. Since only one user is scheduled at any time, the cell throughput is $\sum_{k=1}^{K} C_k$. Let $R_k$ denote the rate reported by user $k$ and let $\tilde{k}$ denote the scheduled user. Then,

$$C_k = \sum_{i=1}^{L} r_i P(R_k = r_i) P(\tilde{k} = k | R_k = r_i). \quad (24)$$

The term $P(R_k = r_i)$ above is determined by the AMC scheme. Specifically, using the approximation in (21), we know that

$$P(R_k = r_i)$$
$$\approx \begin{cases} 1 - B_i \left( e^{-\frac{T_1}{\beta_1}}, a_{1,k}, b_{1,k} \right), & i = 0, \\ B_i \left( e^{-\frac{T_i}{\beta_i}}, a_{i,k}, b_{i,k} \right) \\ \quad - B_i \left( e^{-\frac{T_{i+1}}{\beta_{i+1}}}, a_{i+1,k}, b_{i+1,k} \right), & 1 \le i < L, \\ B_i \left( e^{-\frac{T_L}{\beta_L}}, a_{L,k}, b_{L,k} \right), & i = L. \end{cases} \quad (25)$$

We now evaluate $P(\tilde{k} = k | R_k = r_i)$, which depends on the scheduler. The final expression for $C_k$ then follows directly from (24).

**Result** 5: The term $P(\tilde{k} = k | R_k = r_i)$ for different schedulers is as follows:

1) Greedy scheduler: It is given by (26) at the top of the next page.
2) RR scheduler: $P(\tilde{k} = k | R_k = r_i) = \frac{1}{K}$.
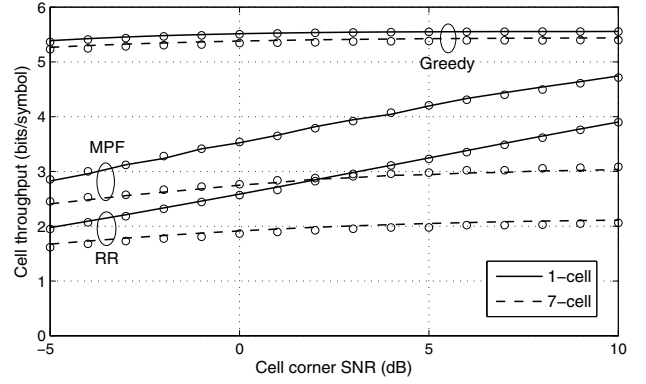3) MPF scheduler: Let $i_{lk}$ be the index of the highest rate



Fig. 8.    LTE: Cell throughput versus cell corner SNR for greedy, RR, and MPF schedulers with and without the presence of interferers for SISO ($K = 10$, $N_{sc} = 24$, $\sigma_{shad} = 8$ dB, $\eta = 3.7$, 512-point FFT, BW = 5 MHz, and TU channel). Simulation results are shown using markers 'o' and analytical results are shown using lines.
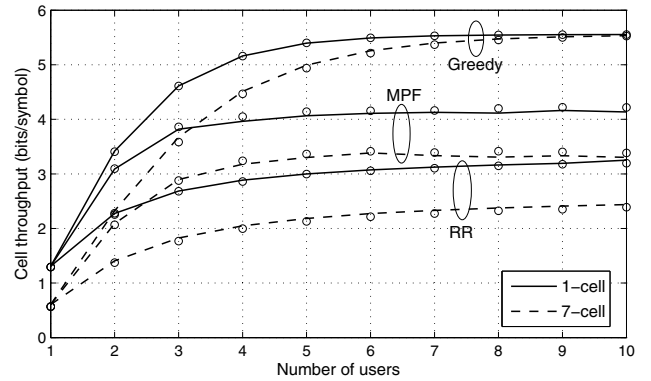


Fig. 9.    LTE: Cell throughput versus number of users in a cell for greedy, RR, and MPF schedulers with and without the presence of interferers for SIMO (Cell corner SNR = 10 dB, $N_{sc} = 24$, $N_r = 2$, $\sigma_{shad} = 8$ dB, $\eta = 3.7$, 512-point FFT, BW = 5 MHz, and TU channel). Simulation results are shown using markers 'o' and analytical results are shown using lines.

that is strictly less than $r_i \frac{\mathbb{E}[R_l]}{\mathbb{E}[R_k]}$. Then,

$$P(k^* = k | R_k = r_i)$$
$$= \prod_{\substack{l=1 \\ l \ne k}}^{K} \left[ 1 - B_i \left( e^{-\frac{T_{i_{lk}+1}}{\beta_{i_{lk}+1}}}, a_{i_{lk}+1,l}, b_{i_{lk}+1,l} \right) \right]. \quad (27)$$

*Proof:* The proof is relegated to Appendix G.    ∎

### B. Numerical Results

Given the large number of possible parameter combinations, we illustrate a sampling of them to study the effect of different antenna modes, schedulers, cell corner SNR, number of users in the cell, and other system parameters. A hexagonal cellular layout is considered with $M = 6$ first-tier interfering BSs. The cell radius $R$ is $10 d_0$. The $k^{th}$ user is placed at a radial distance of $\frac{k}{K} R$ from the serving BS and at an azimuth of $\frac{2\pi k}{K}$. Such a user placement captures the interference variations at different locations in a cell and the non-identical channels seen by different users. Furthermore, $N_{sc} = 24$, $\eta = 3.7$, and $\sigma_{shad} = 8$ dB.

The cell throughput for LTE as a function of the cell corner SNR for $K = 10$ users per cell is plotted in Figure 8 for

$$P(k^* = k | R_k = r_i) = \sum_{p=1}^{K-1} \frac{1}{p+1} \left[ \sum_{\substack{n_1=1 \\ n_1 \neq k}}^{K} \cdots \sum_{\substack{n_p=n_{p-1}+1 \\ n_p \neq k}}^{K} \prod_{q \in \{n_1, \ldots, n_p\}} \left[ B_i \left( e^{-\frac{T_i}{\beta_i}}, a_{i,q}, b_{i,q} \right) - B_i \left( e^{-\frac{T_{i+1}}{\beta_{i+1}}}, a_{i+1,q}, b_{i+1,q} \right) \right] \right.$$

$$\left. \times \prod_{\substack{t=1, t \neq k \\ t \notin \{n_1 \ldots, n_p\}}}^{K} \left[ 1 - B_i \left( e^{-\frac{T_i}{\beta_i}}, a_{i,t}, b_{i,t} \right) \right] \right] + \prod_{\substack{l=1 \\ l \neq k}}^{K} \left[ 1 - B_i \left( e^{-\frac{T_i}{\beta_i}}, a_{i,l}, b_{i,l} \right) \right]. \quad (26)$$

the three schedulers and SISO. We see that the analysis and simulations match well for all the schedulers. In the single cell scenario, in which there is no co-channel interfererence, the throughputs of the RR and MPF schedulers increase almost linearly with the cell corner SNR. The throughput of the greedy scheduler saturates to the highest MCS rate. However, in the multi-cell scenario, the co-channel interference power simultaneously grows with the cell corner SNR. Hence, the throughput increase in the RR and MPF schedulers becomes sub-linear, and the greedy scheduler's throughput saturates to a lower value. The drop in throughput depends on the scheduler. For example, at a cell corner SNR of 5 dB, the drop is 39%, 29%, and 3% for the RR, MPF, and greedy schedulers, respectively. The greedy scheduler exhibits minimal loss as it schedules users closer to the serving BS that are farther away from the interfering BSs.

The cell throughput as a function of $K$, with the cell corner SNR set to 5 dB, is plotted in Figure 9 for SIMO. Notice the excellent match between analysis and simulations. As expected, the throughput improvement is the highest for the greedy scheduler and the lowest for the RR scheduler. Further, the throughput loss due to interference for the greedy scheduler becomes negligible as $K$ increases, which is not the case for the RR and MPF schedulers.

## VI. CONCLUSIONS

We developed a general framework for analyzing the throughput of the optimal link adaptation scheme for an OFDM system in which the packets are sent over multiple subcarriers that see different gains. EESM is used as the link quality metric for AMC. We saw that EESM is well modeled in terms of the Beta distribution for a wide range of subcarrier correlations and for various antenna diversity modes. For a point-to-point link, it led to a tight upper bound and an accurate approximation for the throughput. We then developed closed-form throughput expressions for the multi-cell, multi-user scenario in which multi-user diversity is exploited by a frequency-domain scheduler. Co-channel interference was also modeled and three different schedulers were analyzed.

## APPENDIX

### A. Mean and Variance of $Y_m$ for Independent Subcarriers

The MGF $\Psi_X(t)$ of an RV $X$ is defined as $\Psi_X(t) = \mathbb{E}\left[e^{tX}\right]$. When the $N_{sc}$ subcarrier SNRs are i.i.d., the mean $\mu_m$ and variance $v_m$ of $Y_m$ can be expressed in terms of the MGF of $\gamma_i$ as

$$\mu_m = \Psi_{\gamma_i}\left(-\beta_m^{-1}\right), \quad (28)$$

$$v_m = \frac{1}{N_{sc}} \left( \Psi_{\gamma_i}\left(-2\beta_m^{-1}\right) - \left[\Psi_{\gamma_i}\left(-\beta_m^{-1}\right)\right]^2 \right). \quad (29)$$

Since $\gamma_i = cX_\tau$, where $X_\tau$ is a standard Chi-squared RV with $\tau$ degrees of freedom, it can be shown that its MGF is given by $\Psi_{\gamma_i}(t) = (1 - 2ct)^{-\frac{\tau}{2}}$. Substituting this in (28) and (29) yields (10) and (11), respectively.

### B. Mean and Variance of $Y_m$ for $2 \times 2$ MIMO with Independent Subcarriers

The PDF of $\gamma_i$ is given by $f_{\gamma_i}(x) = \frac{1}{\sigma^2}\left(\left(\frac{x}{\sigma^2}\right)^2 - \frac{2x}{\sigma^2} + 2\right)e^{-\frac{x}{\sigma^2}} - \frac{2}{\sigma^2}e^{-\frac{2x}{\sigma^2}}$, for $x \geq 0$ [8]. Its MGF can then be shown to be $\Psi_{\gamma_i}(t) = \frac{2\left(1+t^2\sigma^4-t\sigma^2\right)}{(1-t\sigma^2)^3} - \frac{2}{2-t\sigma^2}$. Substituting this in (28) and (29) yields (12) and (13), respectively.

### C. Mean and Variance of $Y_m$ for Correlated Subcarriers

The joint MGF of $\boldsymbol{\Gamma}$, $\Psi_{\boldsymbol{\Gamma}}(t_1, \ldots, t_{N_{sc}})$, is defined as $\Psi_{\boldsymbol{\Gamma}}(t_1, \ldots, t_{N_{sc}}) = \mathbb{E}\left[e^{\sum_{i=1}^{N_{sc}} t_i \gamma_i}\right]$. The mean $\mu_m$ and the variance $v_m$ can be expressed in terms of $\Psi_{\boldsymbol{\Gamma}}$ as

$$\mu_m = \Psi_{\boldsymbol{\Gamma}}(t_1, \ldots, t_{N_{sc}})\Big|_{\substack{t_1=-\beta_m^{-1} \\ t_k=0, \text{else}}}, \quad (30)$$

$$v_m = \frac{1}{N_{sc}^2} \left[ \sum_{i=1}^{N_{sc}} \sum_{j=1, j \neq i}^{N_{sc}} \Psi_{\boldsymbol{\Gamma}}(t_1, \ldots, t_{N_{sc}})\Big|_{\substack{t_i, t_j=-\beta_m^{-1} \\ t_k=0, \text{else}}} \right.$$
$$\left. + \sum_{i=1}^{N_{sc}} \Psi_{\boldsymbol{\Gamma}}(t_1, \ldots, t_{N_{sc}})\Big|_{\substack{t_i=-2\beta_m^{-1} \\ t_k=0, \text{else}}} \right] - \mu_m^2. \quad (31)$$

Since the channel gains of the different transmit-receive antenna pairs are i.i.d., $\Psi_{\boldsymbol{\Gamma}}$ simplifies to

$$\Psi_{\boldsymbol{\Gamma}}(t_1, \ldots, t_{N_{sc}}) = \left( \mathbb{E}\left[e^{\mathbf{g}_{11}^{\mathrm{T}} \mathbf{S} \mathbf{g}_{11}}\right] \right)^{\max(N_t, N_r)}, \quad \text{where}$$

$$\mathbf{S} = \sigma^2 \begin{bmatrix} \text{diag}([t_1, \ldots, t_{N_{sc}}]) & \mathbf{0}_{N_{sc}} \\ \mathbf{0}_{N_{sc}} & \text{diag}([t_1, \ldots, t_{N_{sc}}]) \end{bmatrix} \quad \text{and}$$

$\mathbf{g}_{11} = \left[\text{Re}(\boldsymbol{h}_{11})^{\mathrm{T}} \text{Im}(\boldsymbol{h}_{11})^{\mathrm{T}}\right]^{\mathrm{T}}$. Recall that $\boldsymbol{h}_{11}$ is defined in Section III-A2. Since $\mathbf{g}_{11}$ is a zero-mean Gaussian random vector with covariance matrix $\mathbf{K}$, we can show that $\mathbb{E}\left[e^{\mathbf{g}_{11}^{\mathrm{T}} \mathbf{S} \mathbf{g}_{11}}\right] = \det\left(\mathbf{I}_{2N_{sc}} - 2\mathbf{K}\mathbf{S}\right)^{-\frac{1}{2}}$. Substituting $\Psi_{\boldsymbol{\Gamma}}$ in (30) and (31), yields the desired closed-form expressions.

### D. Brief Derivation of Approximation Error

The support of $f_{Y_m}(x)$ is $[0, 1]$, and it is square integrable. The alternative form of the Jacobi polynomials form a complete orthogonal system in $\mathcal{L}^2[0, 1]$, which is the space of all square integrable functions with support in $[0, 1]$, with the weight function $f_{Z_m}(x)$ provided $a_m, b_m > 0$, which is satisfied in our problem. Thus, we can express $f_{Y_m}(x)$ in terms of the alternative form of the Jacobi polynomials as

$$f_{Y_m}(x) = f_{Z_m}(x) \sum_{k=0}^{\infty} c_k G_k(a_m, b_m, x), \qquad (32)$$

where $c_k$ is given in the result statement. Further, $\forall x \in [0, 1]$, $G_0(a_m, b_m, x) = 1$ and $c_0 = 1$. Subtracting $f_{Z_m}(x)$ from (32) yields (17).

### E. Proof of Lemma 1

The derivative of $\gamma_{\text{eff}}$ with respect to (w.r.t.) $\beta$ is given by

$$\frac{d\gamma_{\text{eff}}}{d\beta} = -\log\left(\frac{1}{N_{\text{sc}}} \sum_{i=1}^{N_{\text{sc}}} e^{-\frac{\gamma_i}{\beta}}\right) - \frac{1}{\beta} \sum_{i=1}^{N_{\text{sc}}} \frac{\gamma_i e^{-\frac{\gamma_i}{\beta}}}{\sum_{i=1}^{N_{\text{sc}}} e^{-\frac{\gamma_i}{\beta}}}. \quad (33)$$

To prove the monotonicity of $\gamma_{\text{eff}}$ w.r.t. $\beta$, we need to show that $\frac{d\gamma_{\text{eff}}}{d\beta} \geq 0$, which after some algebraic manipulations, is equivalent to showing that

$$\log(N_{\text{sc}}) \geq -\sum_{i=1}^{N_{\text{sc}}} \tilde{\nu}_i \log(\tilde{\nu}_i), \qquad (34)$$

where $\tilde{\nu}_i = e^{-\frac{\gamma_i}{\beta}}\left(\sum_{j=1}^{N_{\text{sc}}} e^{-\frac{\gamma_j}{\beta}}\right)^{-1}$. Note that $\tilde{\nu}_i$ lies between 0 and 1, and $\sum_{i=1}^{N_{\text{sc}}} \tilde{\nu}_i = 1$. Thus, $\{\tilde{\nu}_i\}_{i=1}^{N_{\text{sc}}}$ is a valid probability mass function, and the term on the right hand side in (34) is its entropy. Since the entropy is less than or equal to the logarithm of the support set's cardinality, (34) follows.

### F. Upper Bound and Approximation for Average Throughput

*Upper bound:* The probability of selecting MCS $m$ is upper bounded by

$$P\left(\gamma_{\text{eff}}^{(m)} \geq T_m, \gamma_{\text{eff}}^{(m+1)} < T_{m+1}, \ldots, \gamma_{\text{eff}}^{(L)} < T_L\right)$$
$$\leq P\left(\gamma_{\text{eff}}^{(m)} \geq T_m, \gamma_{\text{eff}}^{(m+1)} < T_{m+1}\right). \quad (35)$$

Using the ordering property of $\gamma_{\text{eff}}$ in Lemma 1, it follows that

$$P\left(\gamma_{\text{eff}}^{(m)} \geq T_m, \gamma_{\text{eff}}^{(m+1)} < T_{m+1}\right)$$
$$= P\left(T_m \leq \gamma_{\text{eff}}^{(m)} < \gamma_{\text{eff}}^{(m+1)} < T_{m+1}\right),$$
$$\leq \min\left\{P\left(T_m \leq \gamma_{\text{eff}}^{(m)} < T_{m+1}\right),\right.$$
$$\left. P\left(T_m \leq \gamma_{\text{eff}}^{(m+1)} < T_{m+1}\right)\right\}. \quad (36)$$

Equation (36) follows because individually $P\left(T_m \leq \gamma_{\text{eff}}^{(m)} < T_{m+1}\right)$ and $P\left(T_m \leq \gamma_{\text{eff}}^{(m+1)} < T_{m+1}\right)$ are upper bounds. Substituting (36) in (18), and expressing the probabilities in terms of the incomplete Beta function using (9), yields (20).

*Approximation:* We lower bound the expression in (35) as follows. This is an approximation because it lower bounds an upper bound.

$$P\left(\gamma_{\text{eff}}^{(m)} > T_m, \gamma_{\text{eff}}^{(m+1)} < T_{m+1}\right)$$
$$= P\left(\gamma_{\text{eff}}^{(m)} > T_m\right) - P\left(\gamma_{\text{eff}}^{(m)} > T_m, \gamma_{\text{eff}}^{(m+1)} > T_{m+1}\right),$$
$$\geq P\left(\gamma_{\text{eff}}^{(m)} > T_m\right) - P\left(\gamma_{\text{eff}}^{(m+1)} > T_{m+1}\right). \quad (37)$$

Substituting (37) in (18), and expressing the probabilities in terms of the incomplete Beta function using (9), yields (21).

### G. $P(\tilde{k} = k | R_k = r_i)$ for Different Schedulers

*1) Greedy Scheduler:* User $k$ is scheduled if one of the following two mutually exclusive events occurs: (i) the reported rate of user $k$ is higher than that of every other user, or (ii) user $k$ and $p$ other users, $1 \leq p \leq K - 1$, report the same highest rate, and the breaking of ties among these users results in user $k$ being selected. Let $\{R_\Lambda = r_i\}$ denote the event that all the users in the set $\Lambda$ report rate $r_i$, let $|\Lambda|$ denote the cardinality of the set $\Lambda$, and let $\Lambda^c$ denote its complement. Hence,

$$P(k^* = k | R_k = r_i) = P(R_l < R_k, \forall l \neq k | R_k = r_i)$$
$$+ \sum_{p=1}^{K-1} \frac{1}{p+1} \sum_{\substack{\Lambda \subset \{1,\ldots,K\}\setminus\{k\} \\ |\Lambda|=p}} P(R_\Lambda = r_i, R_{\Lambda^c} < r_i | R_k = r_i).$$
$$(38)$$

Since the rates reported by the users are independent, we get

$$P(k^* = k | R_k = r_i) = \prod_{l=1, l\neq k}^{K} P(R_l < r_i)$$
$$+ \sum_{p=1}^{K-1} \frac{1}{p+1} \left( \sum_{\substack{n_1=1 \\ n_1\neq k}}^{K} \cdots \sum_{\substack{n_p=n_{p-1}+1 \\ n_p\neq k}}^{K} \left[ \prod_{q\in\{n_1,\ldots,n_p\}} P(R_q = r_i) \right] \right.$$
$$\left. \times \left[ \prod_{t=1, t\notin\{k,n_1,\ldots,n_p\}}^{K} P(R_t < r_i) \right] \right). \quad (39)$$

Writing the probability terms in (39) in terms of the incomplete Beta function yields (26).

*2) RR Scheduler:* The RR scheduler does not use the reported rate. Hence, $P(\tilde{k} = k | R_k = r_i) = P(\tilde{k} = k) = \frac{1}{K}$.

*3) MPF Scheduler:* User $k$ is scheduled if its MPF metric, which is a real-valued RV, exceeds that of every other user. Hence,[3]

$$P(\tilde{k} = k | R_k = r_i) = P\left(\frac{R_l}{\mathbb{E}[R_l]} < \frac{R_k}{\mathbb{E}[R_k]}, \forall l \neq k | R_k = r_i\right),$$
$$= \prod_{\substack{l=1 \\ l\neq k}}^{K} P(R_l \leq r_{i_{lk}}), \qquad (40)$$

where $r_{i_{lk}}$ is defined in the result statement. To arrive at the above expression in (40), we used the fact that the rates reported by the users are independent. Writing the probability terms in terms of the incomplete Beta function yields (27).

---

[3]We do not consider the the event in which the real-valued MPF metrics of two users are the same, since it occurs with zero probability.

## REFERENCES

[1] S. Simoens, S. Rouquette-Léveil, P. Sartori, Y. Blankenship, and B. Classon, "Error prediction for adaptive modulation and coding in multiple-antenna OFDM systems," *Signal Process.*, vol. 86, no. 8, pp. 1911–1919, Aug. 2006.

[2] A. J. Goldsmith, *Wireless Communications*, 1st ed. Cambridge University Press, 2005.

[3] S. S. Tsai and A. C. K. Soong, "Effective-SNR mapping for modeling frame error rates in multiple-state channels," 3GPP2, Tech. Rep. 3GPP2-C30-20030429-010, 2003.

[4] E. Westman, "Calibration and evaluation of the exponential effective SINR mapping (EESM) in 802.16," Master's thesis, The Royal Institute of Technology (KTH), Stockholm, Sweden, Sept. 2006.

[5] K. Brueninghaus, D. Astely, T. Salzer, S. Visuri, A. Alexiou, S. Karger, and G.-A. Seraji, "Link performance models for system level simulations of broadband radio access systems," in *Proc. 2005 PIMRC*, pp. 2306–2311.

[6] "Feasibility study for OFDM for UTRAN enhancement," 3GPP, Tech. Rep. 25.892 v2.0.0 (2004-06), 2004.

[7] R. Srinivasan, J. Zhuang, L. Jalloul, R. Novak, and J. Park, "IEEE 802.16m evaluation methodology document (EMD)," Tech. Rep. IEEE 802.16m-08/004r2, 2008.

[8] S. N. Donthi and N. B. Mehta, "An accurate model for EESM and its application to analysis of CQI feedback schemes and scheduling in LTE," *IEEE Trans. Wireless Commun.*, vol. 10, no. 10, pp. 3436–3448, Oct. 2011.

[9] H. Song, R. Kwan, and J. Zhang, "Approximations of EESM effective SNR distribution," *IEEE Trans. Commun.*, vol. 59, no. 2, pp. 603–612, Feb. 2011.

[10] J. Fan, Q. Yin, G. Y. Li, B. Peng, and X. Zhu, "MCS selection for throughput improvement in downlink LTE systems," in *Proc. 2011 ICCCN*, pp. 1–5.

[11] D. Ben Cheikh, J. M. Kelif, M. Coupechoux, and P. Godlewski, "Analytical joint processing multi-point cooperation performance in Rayleigh fading," *IEEE Commun. Lett.*, vol. 1, no. 4, pp. 272–275, Aug. 2012.

[12] A. Papoulis, *The Fourier Integral and Its Applications*, 1st ed. Mcgraw-Hill, 1962.

[13] J.-G. Choi and S. Bahk, "Cell-throughput analysis of the proportional fair scheduler in the single-cell environment," *IEEE Trans. Veh. Technol.*, vol. 56, no. 2, pp. 766–778, Mar. 2007.

[14] T. Jiang, L. Song, and Y. Zhang, *Orthogonal Frequency Division Multiple Access Fundamentals and Applications*, 1st ed. Auerbach Publications, 2010.

[15] S. Kant and T. L. Jensen, "Fast link adaptation for IEEE 802.11n," Master's thesis, Aalborg Univ., Denmark, Feb. 2007.

[16] T. L. Jensen, S. Kant, J. Wehinger, and B. H. Fleury, "Fast link adaptation for MIMO OFDM," *IEEE Trans. Veh. Technol.*, vol. 59, no. 8, pp. 3766–3778, Oct. 2010.

[17] T. Tao and A. Czylwik, "Performance analysis of link adaptation in LTE systems," in *Proc. 2011 Int. ITG Workshop Smart Antennas*, pp. 1–5.

[18] Y. Huang and B. D. Rao, "An analytical framework for heterogeneous partial feedback design in heterogeneous multicell OFDMA networks," *IEEE Trans. Signal Process.*, vol. 61, no. 3, pp. 753–769, Feb. 2013.

[19] R. Giuliano and F. Mazzenga, "Dimensioning of OFDM/OFDMA-based cellular networks using exponential effective SINR," *IEEE Trans. Veh. Technol.*, vol. 58, no. 8, pp. 4204–4213, Oct. 2009.

[20] K. Sayana, J. Zhuang, and K. Stewart, "Link performance abstraction based on mean mutual information per bit (MMIB) of the LLR channel," Tech. Rep. IEEE C802.16m-07/097, May 2007.

[21] X. Qiu and J. Chuang, "Link adaptation in wireless data networks for throughput maximization under retransmissions," in *Proc. 1999 ICC*, pp. 1272–1277.

[22] I. S. Gradshteyn and I. M. Ryzhik, *Table of Integrals, Series and Products*, 4th ed. Academic Press, 1980.

[23] M. R. McKay, I. B. Collings, and P. J. Smith, "Capacity and SER analysis of MIMO beamforming with MRC," in *Proc. 2006 ICC*, pp. 1326–1330.

[24] G. Fishman, *Monte Carlo: Concepts, Algorithms, and Applications*, 1st ed. Springer, 1996.

[25] T. D. Pham and K. G. Balmain, "Multipath performance of adaptive antennas with multiple interferers and correlated fadings," *IEEE Trans. Veh. Technol.*, vol. 48, no. 2, pp. 342–352, Mar. 1999.

[26] S. B. Provost, "Moment-based density approximants," *The Mathematica J.*, vol. 9, no. 4, pp. 727–756, Aug. 2005.

[27] G. L. Stüber, *Principles of Mobile Communications*, 3rd ed. Kluwer Academic Publishers, 1996.

[28] N. Beaulieu and Q. Xie, "An optimal lognormal approximation to lognormal sum distributions," *IEEE Trans. Veh. Technol.*, vol. 53, no. 2, pp. 479–489, Mar. 2004.

[29] A. Papoulis, *Probability, Random Variables and Stochastic Processes*, 3rd ed. McGraw Hill, 1991.

[30] S. Sesia, I. Toufik, and M. Baker, *LTE – The UMTS Long Term Evolution, From Theory to Practice*, 1st ed. John Wiley and Sons, 2009.

[31] "Universal mobile telecommunications system (UMTS); deployment aspects," 3GPP, Tech. Rep. 25.943 v6.0.0 (2004-12), 2004.

[32] S.-H. Hur and B. Rao, "Sum rate analysis of a reduced feedback OFDMA downlink system employing joint scheduling and diversity," *IEEE Trans. Signal Process.*, vol. 60, no. 2, pp. 862–876, Feb. 2012.

[33] A. Jalali, R. Padovani, and R. Pankaj, "Data throughput of CDMA-HDR a high efficiency-high data rate personal communication wireless system," in *Proc. 2000 VTC – Spring*, pp. 1854–1858.

**Jobin Francis** received his Bachelor of Technology degree in Electronics and Communication Eng. from the College of Engineering, Trivandrum, India in 2009 and his Master of Engineering degree in Signal Processing from the Indian Institute of Science (IISc), Bangalore in 2011. He is currently pursuing his Ph.D. in the Dept. of Electrical Communication Eng. at IISc. His research interests include adaptive modulation and coding, resource allocation in OFDM, and design and analysis of wireless cellular systems.

**Neelesh B. Mehta** (S'98-M'01-SM'06) received his Bachelor of Technology degree in Electronics and Communications Eng. from the Indian Institute of Technology (IIT), Madras in 1996, and his M.S. and Ph.D. degrees in Electrical Eng. from the California Institute of Technology, Pasadena, USA in 1997 and 2001, respectively. He is now an Associate Professor in the Dept. of Electrical Communication Eng., Indian Institute of Science (IISc), Bangalore. Before joining IISc in 2007, he was a research scientist in USA from 2001 to 2007 in AT&T Laboratories, NJ, Broadcom Corp., NJ, and Mitsubishi Electric Research Laboratories (MERL), MA.

His research includes work on link adaptation, multiple access protocols, cellular systems, MIMO and antenna selection, cooperative communications, energy harvesting networks, and cognitive radio. He was also actively involved in the Radio Access Network (RAN1) standardization activities in 3GPP from 2003 to 2007. He is an Editor of IEEE WIRELESS COMMUNICATIONS LETTERS, IEEE TRANSACTIONS ON COMMUNICATIONS, and the *Journal of Communications and Networks*. He currently serves as the Director of Conference Publications on the Board of Governors of IEEE ComSoc.